Supplement of The Cryosphere, 10, 1361–1380, 2016
http://www.the-cryosphere.net/10/1361/2016/
doi:10.5194/tc-10-1361-2016-supplement

The Cryosphere Open Access EGU

Supplement of

Mapping snow depth in open alpine terrain from stereo satellite imagery

R. Marti et al.

Correspondence to: S. Gascoin (simon.gascoin@cesbio.cnes.fr)

Contents

1 Study site

Fig. 1) shows the land cover map of Bassies catchment.

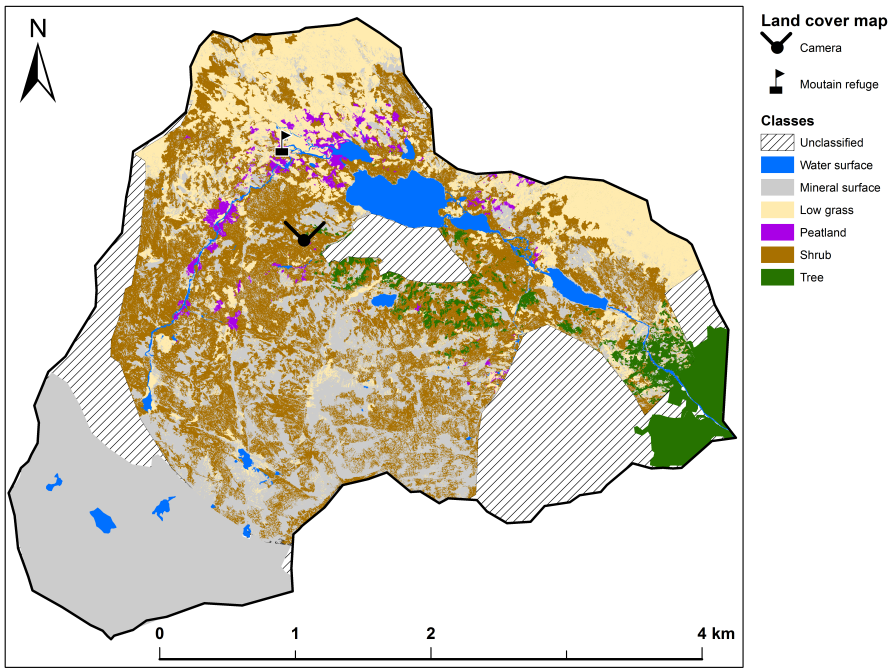

Figure 1: Land cover map of Bassies catchment.

2 Photogrammetric processing

2.1 ASP's parameters used to generate the DEMs from the Pleiades images.

We present in the following table the parameter set used to treat the flow of data through the Stereo Pipeline.

Stage	Parameter set	Selected parameter
Registration	ISIS adjust	No bundle adjustment
Stereo pre-processing	Pre-alignment options	Affine epipolar
	Intensity Normalization	Use entire input range
	Preprocessing filter	Laplacian of Gaussian
	Kernel size	prefilter-kernel-width 1.4
	Correlation Seed Mode	from disparity map
	Correlation number of pyramids	corr-max-levels 3
	Correlation sub seed value	corr-sub-seed-percent 0.25
Disparity map initialization	cost function	normalized cross correlation
	correlation kernel size	corr-kernel 25 25
	correlation window size	corr-search -80 -2 20 2
	Correlation time out	corr-timeout 600
Sub-pixel refienement	subpixel modes	affine window
	correlation kernel size	kernel 35 35
Outlier rejection / Hole filling	Fill in holes with an inpainting method	disable-fill-holes
	Automatic "erode" low confidence pixels	filter mode 1
		rm-half-kernel 5 5
		max-mean-diff 3
		rm-min-matches 60
		rm-threshold 3
Stereo triangulation	near-universe-radius	0.0
	far-universe-radius	0.0

2.2 Raw cloud from the snow-free Pleiades triplet

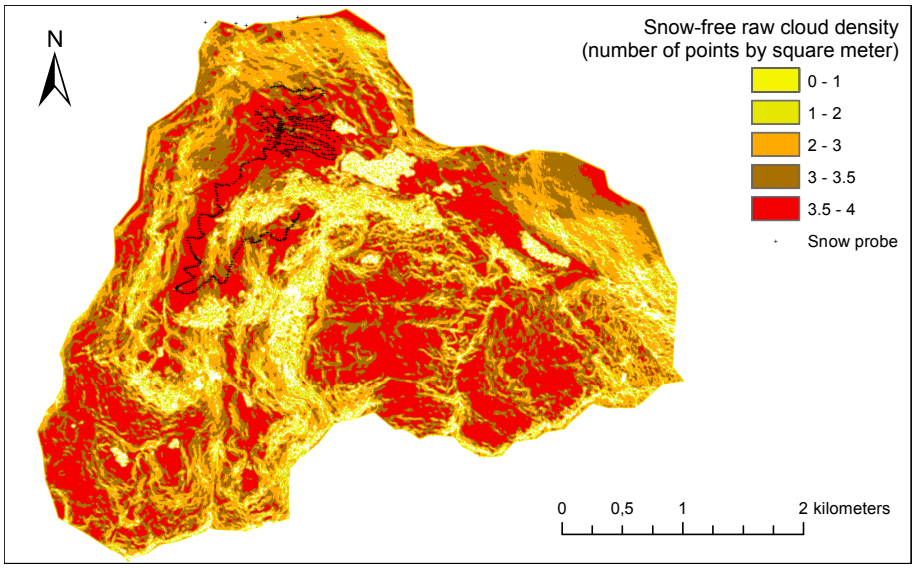

Figure 2: Density of the point cloud generated from the snow-free Pleiades triplet image (number of points per square meter).

2.3 Raw cloud from the winter Pleiades triplet

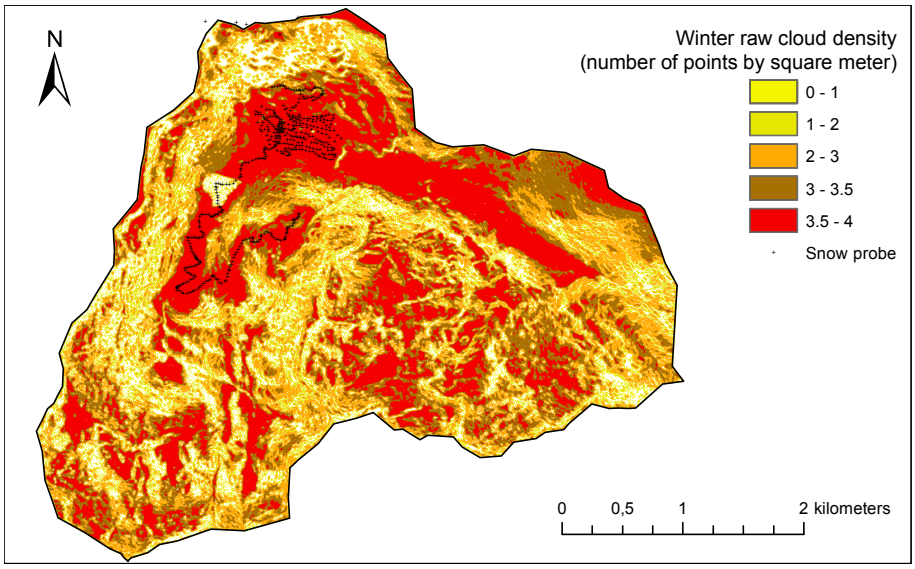

Figure 3: Density of the point cloud generated from the winter Pleiades triplet image (number of points per square meter).

3 Random error assessments

The random error on the DGPS measurements were provided during the post-treatment step by the GPS Pathfinder office software (V. 5.4). Such estimations are based on the GDOP (Geometrical Dilution of Precision) associated to the positions and the distance to the correction base (21 km in our study). The random error associated to the probe measurements are mainly due to penetration of the probe tip into the snow substrate, the reading between two probe spacing, and the verticality of the snow probe. According to the error propagation law, the random errors terms due to the DGPS and the snow-probe measurements were estimated as follows:

- random error term due to the DGPS measurements: $\sigma_{DGPS} = 0.1\ m$
- random error term due to the probe measurements: $\sigma_{probe} = 0.15\ m$
- random error term due to the DGPS and the snow-probe measurements:

$$\sigma_{DGPS+probe} = \sqrt{\sigma^2_{DGPS} + \sigma^2_{probe}} = \sqrt{0.1^2 + 0.15^2} = 0.18\ m. \quad (1)$$

We estimated the random error in the 2m-DEMs and the 2m-dDEMS based on the SD of the residuals terms (equation (1), (3) and (4) from section 4.1) as follows:

- 2m-Pléiades Winter DEM:

$$\sigma_{Zwinter} = \sqrt{SD^2_{R_{Z_w}} - \sigma^2_{DGPS}} = \sqrt{0.32^2 - 0.1^2} = 0.31\ m. \quad (2)$$

- 2m-Pléiades Snow-free DEM:

$$\sigma_{Zsnow-free} = \sqrt{SD^2_{R_{Z_s}} - \sigma^2_{DGPS} - \sigma^2_{probe}} = \sqrt{0.66^2 - 0.1^2 - 0.15^2} = 0.63\ m. \quad (3)$$

- 2m-Pléiades dDEM:

$$\sigma_{2m-dDEMPlei} = \sqrt{SD^2_{2m-\Delta Z\ Plei} - \sigma^2_{probe}} = \sqrt{0.58^2 - 0.15^2} = 0.56\ m \quad (4)$$

- 2m-UAS dDEM:

$$\sigma_{2m-dDEMUAS} = \sqrt{SD^2_{2m-\Delta Z\ UAS} - \sigma^2_{probe}} = \sqrt{0.62^2 - 0.15^2} = 0.60\ m \quad (5)$$

- 2m-Pléiades and UAS dDEMS differencing:

$$\sigma_{2m-\Delta(\Delta Z)} = \sqrt{\sigma^2_{2m-\Delta Z\ Plei} + \sigma^2_{2m-\Delta Z\ UAS}} = \sqrt{0.56^2 + 0.60^2} = 0.82\ m \quad (6)$$

4 Supplementary table

In the case where the Pléiades dDEM pixel values were higher than the maximum snow-probe value, $HS_{\max}$ (50 occurrences), the dDEM values are 40 to 50% of the cases also above this threshold. Even if the true HS is unknown, the mean of $|\Delta Z - HS_{\max}|_{HS_{\max}<\Delta Z}$ may be taken as an indication that the dDEM values are not inconsistent at this locations. The mean difference to the threshold value when the dDEM is below is 0.64 m.

In the case where the UAV dDEM pixel values were higher than the maximum snow-probe value, $HS_{\max}$ (32 occurrences), 81% of the UAV dDEM values are also above this threshold. The mean of $|\Delta Z - HS_{max}|_{HS_{max}<\Delta Z}$ varies from 0.57 to 0.69 m, according to the drone dDEM pixel resolution.

Table 1: Percentage of dDEM pixel values which exceed the maximum snow-probe value ($HS_{\max}$, 2.2 m and 3.2 m respectively, according to the type of the snow-probe). We also calculated the mean of the absolute difference between the dDEM value and $HS_{\max}$, in the cases where the pixel values were higher than $HS_{\max}$

Data source	Pléiades dDEM pixel size	Number of snow probe	Percentage of $\Delta Z > HS_{\max}$	Mean of $\lvert\Delta Z - HS_{\max}\rvert_{HS_{\max}<dDEM}$
Pléiades tri-stereo	1 m	50	50%	0.66 m
	2 m		40%	0.68 m
	4 m		40%	0.59 m
UAV	0.1 m	32	81%	0.69 m
	1 m		81%	0.57 m
	2 m		81%	0.66 m

Table 2: VHR optical (civil) satellites that have stereo capabilities comparable to Pléiades, i.e. that could be used for HS mapping based on the same method.(P) means panchromatic, (XS) means multispectral. The ˚symbol, is the temporal resolution column, refers to the angle relative to the off nadir look (in degree). GSD means Ground Sample Distance.

Satellite platform (launch date)	Stereo-capability	Swath width at nadir (km)	Temporal resolution (day)	Spectral resolution (nm)	Radiometric resolution (bits)	Spatial resolution at nadir
Pléiades 1A and 1B (2011 and 2012)	Tri and stereo	20 km	1 day with both Pléiades satellites	480–830 nm	12 bits	0.70 m (P) 2.50 m (XS)
GeoEye-1 (2008)	stereo	15.2 km	2.8 days at 28˚ 8.3 days at 10˚	450–800 nm	11 bits	0.46 m (P) 1.84 m (XS)
WorldView-1 (2007)	stereo	17.7 km	1.7 days at 1 m GSD 5.4 days at 20˚(0.52 m GSD)	400–900 nm	11 bits	0.50 m (P)
WorldView-2 (2009)	stereo	16.4 km	1.1 days at 1 m GSD 3.7 days at 20˚(0.52 m GSD)	450–800 nm	11 bits	0.46 m (P) 1.85 m (XS)
WorldView-3 (2014)	stereo	13.1 km	1 day at 1 m GSD 4.5 days at 20˚.	450–800 nm	11 bits	0.31 m (P) 1.24 m (XS)
SPOT 6 and 7 (2012 and 2014)	Tri and stereo	60 km	1 day with both SPOT satellites	450–745 nm	12 bits	1.50 m (P) 6.00 m (XS)

Table 3: Overview of remote–sensing techniques which can be used to map snow depth. The spatial resolution, spatial extent, and given accuracies should be interpreted as "typical values" generally observed in the literature (e.g. (Dietz et al., 2012; Deems et al., 2013; Nolan et al., 2015; Bühler et al., 2015; Harder et al., 2016; Bühler et al., 2016)).

Remote–sensing techniques	Spatial resolution (m)	Spatial extent (km^2)	Random error in HS mapping (m)	Snow-mapping context & *suitable applications*
Airborne Lidar	0.30 – 2 m	5 – 100s km^2	0.10 – 0.30 m	Thin and thick snow-pack (> 0.30 m) including over forested areas *Spatially distributed SWE* *Avalanche danger mapping* *Input for hydrological model*
Airborne photogrammetry				
" from manned airplane	0.10 – 2 m	5 – 100s km^2	0.10 – 0.30 m	Thin and thick snow-pack (> 0.30 m) *Spatially distributed SWE* *Avalanche danger mapping* *Input for hydrological model*
" from UAV system	0.05 – 2 m	0.1 –5 km^2	0.08 – 0.20 m	Thin and thick snow-pack (> 0.30 m) Sites well connected with transports *Ablation monitoring by multi-temporal acquisitions* *Very fine-scaled snow features monitoring* *Spatially distributed SWE of very small watershed*
Satellite				
" photogrammetry	1–2 m	10 –1500 km^2	0.50 – 0.70 m	Thick snow-pack (> 2 m) *Spatially distributed SWE at snow-peak* *Input for hydrological model* *Snow-accumulation mapping over glaciers*
" passive micro-wave	10 – 25 km	1000s km^2 – global	0.05 – 0.50 m	Thin prairie "dry" snow-pack (< 1 m) or large plateau thin snow-pack *Spatially distributed SWE of cold, thin snow in areas with simple topography even in cloudy conditions*
" radar	10 – 30 m	1000s km^2	potentially subdecimetric	Prairie and alpine snow-pack *Spatially distributed SWE* *even in cloudy conditions* *(only in a research context up to now and with limited success due to inappropriate frequencies)*

References

Bühler, Y., Marty, M., Egli, L., Veitinger, J., Jonas, T., Thee, P., and Ginzler, C.: Snow depth mapping in high-alpine catchments using digital photogrammetry, The Cryosphere, 9, 229–243, doi:10.5194/tc-9-229-2015, 2015.

Bühler, Y., Adams, M. S., Bösch, R., and Stoffel, A.: Mapping snow depth in alpine terrain with unmanned aerial systems (UAS): potential and limitations, The Cryosphere Discussions, pp. 1–36, doi:10.5194/tc-2015-220, 2016.

Deems, J. S., Painter, T. H., and Finnegan, D.: Lidar measurement of snow depth: a review, Journal of Glaciology, 59, 467–479, doi:10.3189/2013JoG12J154, 2013.

Dietz, A. J., Kuenzer, C., Gessner, U., and Dech, S.: Remote sensing of snow - a review of available methods, International Journal of Remote Sensing, 33, 4094–4134, doi:10.1080/01431161.2011.640964, 2012.

Harder, P., Schirmer, M., Pomeroy, J., and Helgason, W.: Accuracy of snow depth estimation in mountain and prairie environements by an unmanned vehicle, The Cryosphere Discussions, pp. 1–22, doi:10.5194/tc-2016-9, 2016.

Nolan, M., Larsen, C., and Sturm, M.: Mapping snow depth from manned aircraft on landscape scales at centimeter resolution using structure-from-motion photogrammetry, The Cryosphere, 9, 1445–1463, doi:10.5194/tc-9-1445-2015, 2015.